

Effect of Interfacial Defects on the Electronic Properties of MoS₂ Based Lateral T-H Heterophase Junctions

Mohammad Bahmani^{1,†}, Mahdi Ghorbani-Asl^{2,‡}, and Thomas Frauenheim^{*,1,3,4}

¹ *Bremen Center for Computational Materials Science (BCCMS), Department of Physics, Bremen University, 28359 Bremen, Germany*

² *Institute of Ion Beam Physics and Materials Research, Helmholtz-Zentrum Dresden-Rossendorf, 01328 Dresden, Germany*

³ *Beijing Computational Science Research Center (CSRC), 100193 Beijing, China*

⁴ *Shenzhen JL Computational Science and Applied Research Institute, 518110 Shenzhen, China*

The coexistence of semiconducting (2H) and metallic (1T) phases of MoS₂ monolayers have further pushed their strong potential for applications in the next generation of electronic devices based on the two-dimensional lateral heterojunctions. Structural defects have considerable effects on the properties of these 2D devices. In particular, the interfaces of two phases are often imperfect and may contain numerous vacancies created by phase engineering techniques, e.g. under the electron beam. Here, the transport behaviors of the heterojunctions in the existence of point defects are explored by means of first-principles calculations and non-equilibrium Green's function approach. While vacancies in semiconducting MoS₂ act as scattering centers, their presence at the interface improves the flow of the charge carriers. In the case of V_{Mo} , the current has been increased by two orders of magnitude in comparison to the perfect device. The enhancement of transmission was explained by changes in the electronic densities at the T-H interface, which open new transport channels for electron conduction.

[†] mbahmani@uni-bremen.de, [‡] mahdi.ghorbani@hzdr.de, ^{*} frauenheim@uni-bremen.de

1 Introduction

Among the developing family of two-dimensional (2D) materials, transition metal dichalcogenides (TMDs) provide one of the most diverse electronic properties including topological insulators, semiconductors, (semi)metals and superconductors [1–3]. Noticeably, such a difference in the electronic structure of TMDs correlates with their structural configurations, called phases [4]. Monolayers of MoS₂ in H-phase, with trigonal prismatic coordination of metal atoms is a semiconducting material [5, 6], while T-phase with octahedral coordination shows metallic character. The H-phase monolayer is reported to be a promising material for field-effect transistors (FETs) with small-scale channel lengths and negligible current leakage [5, 6].

Recent experiments have already shown controlled transitions from one phase to another via external stimuli such as electron beam [7], ion intercalation [8], or laser irradiation [9]. These phase-engineered 2D materials with minimum variations in atomic structure and uniform stoichiometry not only demonstrate rich physical behavior but also open up new avenues for the design of electronic devices. The fabrication of lateral metallic/semiconducting heterostructures has been suggested as a practical method to minimize the contact resistance at the interface between 2D semiconductors and metal electrodes. In particular, the formation of covalent bonds between the two phases can introduce paths for carriers to travel across the interfaces, thus, the Schottky barrier and contact resistance are reduced [10–13]. It has also been demonstrated that 1T-phase engineered electrodes in MoS₂ based electronic devices would generate ohmic contacts and, as a result, improve electrical characteristics [12, 14].

Apart from intrinsic defects, the local phase transitions induced by electron beam irradiation may give rise to the formation of point defects, in particular at the interface of the two phases. [15–22]. Defects can also be intentionally introduced during the post-growth stage via ion bombardment, plasma treatment, vacuum annealing, or chemical etching.[15–22]. Indeed, the theoretical and experimental results showed that the presence of sulfur vacancies can decrease the energy difference between the H and T phases and eventually stabilize the 1T phase in MoS₂ monolayer [23, 24]. The presence of point defects in semiconducting MoS₂ monolayers leads to the observation of the localized states in their electronic structure, which act as short-ranged scattering centers for charge carriers [25–28]. Hence, defects were

found to deteriorate the mobility of the fabricated devices [29–31]. It was also shown that sulfur line vacancies in MoS₂ can behave like pseudo-ballistic wire for electron transport [32].

So far, several theoretical studies have reported the transport properties of phase-engineered devices based on TMDs monolayers including MoS₂ based lateral junctions [11, 12, 33–36]. In most of these studies, however, it is assumed that two phases have a perfect crystalline structure and connected via an atomically sharp and defect-free interface.

Here, transport properties of devices based on MLs MoS₂, containing various point vacancies and antisites at the interface between metallic and semiconducting phases, are the subject of the present study. Our systematic investigations show significant improvements in the current, as molybdenum vacancy and vacancy complexes are created at the interfaces of two phases. These findings render defect engineering as an efficient route to further improve the performance of the devices based on the lateral heterojunctions formed from TMDs.

2 Computational Details

Density-functional theory (DFT) calculations were performed using numerical atomic orbitals (NAOs) basis sets as implemented in SIESTA code [37, 38]. The norm-conserving pseudopotentials, including the effect of core electrons, are employed, which were obtained using the Troullier-Martin method [39, 40]. The Perdew-Burke-Ernzerhof (PBE) functional in the generalized gradient approximation (GGA) is used to describe the exchange and correlation interactions [41].

In the optimization calculations, the Brillouin zone (BZ) of supercells was sampled using a $9 \times 1 \times 3$ MonkhorstPack grid. In the electronic and transport calculations, 5 and 29 k-points were used, respectively, along the transverse direction. The conjugate-gradients (CG) method was applied to optimize the lattice vectors and atomic positions of all the structures and interfaces. The geometries were considered relaxed when the Hellman-Feynman forces on each atom became smaller than 10 meV/Å. The energy cut-off of 450 Ry is used in the framework of the real-space grid techniques to obtain Hartree, exchange, and correlation energies. The Split-Norm was set to 0.16 and the Energy-Shift of 0.02 Ry was chosen to determine the confinement radii. The total energy convergency criteria (ΔE_{tot}) is chosen

to be 10^{-5} eV for k-points and 10^{-4} eV for energy cut-off. When the difference between two consecutive steps was less than 10^{-4} eV, the total energies in self-consistent field (SCF) cycles were considered converging.

The electron transport calculations were performed using non-equilibrium Greens functions (NEGF) techniques, as implemented in TranSIESTA and TBtrans [42, 43]. The same basis sets as for the electronic calculations, namely SZP, were employed for the transport calculations. The current through the heterophase junction under a finite bias voltage was calculated within the Landauer formula [44]

$$I = \frac{2e}{h} \int \text{Trace} \left[G_C^\dagger(E) \Gamma_R(E) G_C(E) \Gamma_L(E) \right] (f_L(E) - f_R(E)) dE. \quad (1)$$

Where $G_C^\dagger(E)$ and $G_C(E)$ are the retarded and advanced Green's functions of the channel region. The effect of left (L) and right (R) electrodes are projected onto the scattering region via their corresponding self-energies, $\Gamma_L(E)$ and $\Gamma_R(E)$. The Fermi distribution of $f_L(E)$ and $f_R(E)$ represent the available states for electrons in the left and right electrodes. The transport calculations were performed at 300 K.

3 Results and Discussion

Depending on the edge orientation of monolayers, armchair and zigzag interfaces can be realized. The armchair interfaces have been shown to be most stable against buckling [11, 34]. They are also energetically more favorable than connecting the zigzag terminated edges in the sulfur-rich limit [33, 34]. The recent theoretical study showed that the conductivity of the armchair edges is higher than the zigzag interfaces due to the presence of metallic Mo zigzag chains along the transport direction [11]. Accordingly, we consider the armchair interface in the present study. In order to create Schottky contacts at the interfaces, the semiconducting 2H-phase of MoS₂ (channel region) is sandwiched between two metal electrodes of 1T-MoS₂, as shown in Fig. 1.

The size of the whole device is 117.50 Å along the transport direction (Z axis) and 22.00 Å in the transverse direction (X axis), including the channel with a length of 98.46 Å

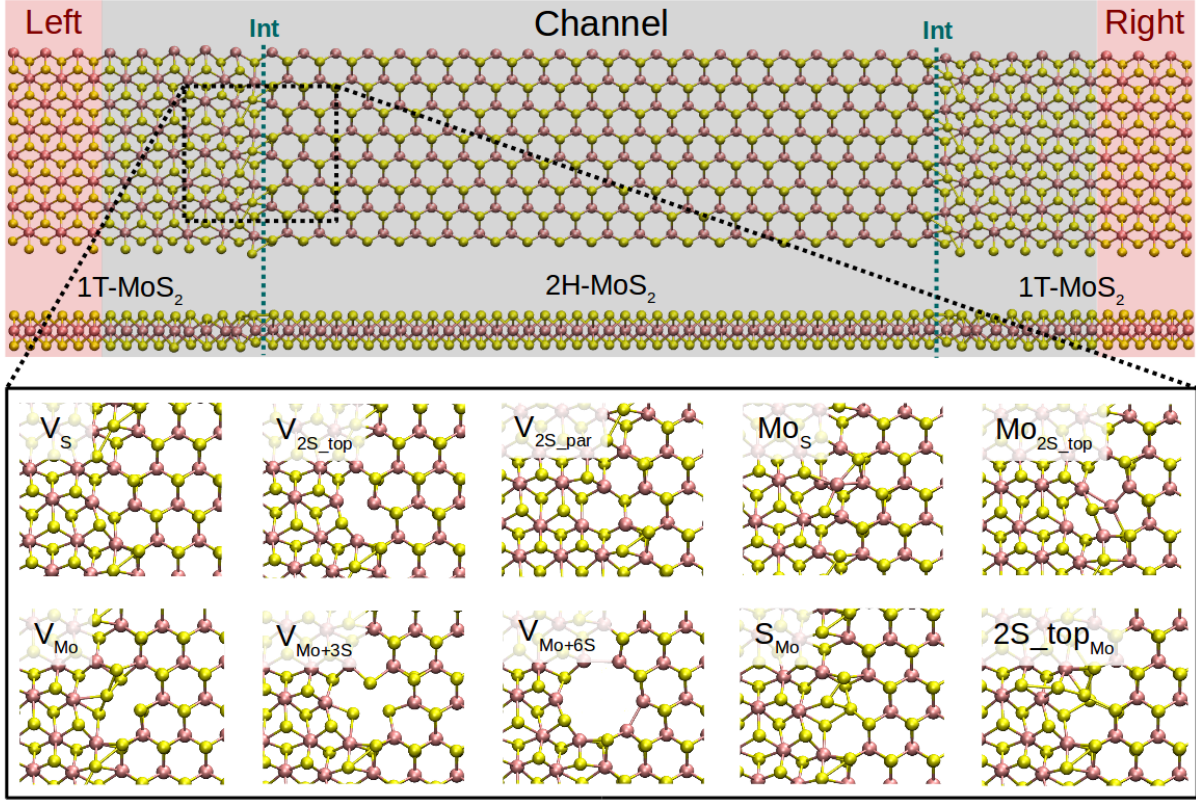


Figure 1: Upper: Schematic of the T-H heterophase junction of MoS₂ monolayer. Electrodes (only 1T-MoS₂) and channel region (a combination of 1T- and 2H-MoS₂) are highlighted with shaded red and black, respectively. The interfaces are indicated with green dashed-lines. Lower: Optimized structures of the point defects at the left interface of the devices are shown. The complete defective devices are shown in Fig. S1 in the supplementary information.

corresponding to 31 unit cells of MoS₂. The channel length is long enough to avoid artificial interactions between the two electrodes. Also, it includes small adjacent portions of the 1T phase as buffer layers to provide a computationally convenient configuration for calculating self-energies at the boundaries.[45]. The periodic boundary conditions were applied along the axis transverse to the transport direction. A vacuum layer of 50 Å normal to the monolayers was considered, which prevents interactions between adjacent supercells.

Several junctions composed of 1T and 2H of MLs MoS₂ are considered without defects (perfect) and when containing point defects in the phase boundaries, as shown in Fig. 1. We considered 10 types of point defects, most of which were observed in experiments [16,

17, 19, 20, 46, 47] and their stability were analyzed by DFT calculations [15, 27, 28, 48]. We look at a sulfur and a molybdenum vacancy, V_S and V_{Mo} , a double sulfur vacancy from upper and bottom layers V_{2S-top} , and the case of removing two atoms from the upper sulfur layer and parallel to the interface, V_{2S-par} . Besides, vacancy complexes of molybdenum and three sulfurs (V_{Mo+3S}) and six sulfurs (V_{Mo+6S}) are also studied. Four antisites are also considered: Mo_S , Mo_{2S-top} , S_{Mo} , and $2S-top_{Mo}$. Our electronic structure calculations indicate that 2H-MoS₂ is a semiconductor with a bandgap of 1.73 eV, while 1T-MoS₂ has a metallic character (see Fig. S2). These results are in agreement with previous theoretical reports at the same level of theory [6, 48-51]. Such studies have shown no difference or a difference of %0.63 between the lattice constant of the T- and H- phase of MoS₂ monolayers. Therefore, the same lattice parameters, namely 3.176Å, are used for both phases. Such a phase transition can be seen as the collective displacement of sulfur atoms while the stoichiometry of the materials is preserved. The constructed lateral heterostructures with armchair edges are optimized, as shown at the top of Fig. 1. It should be noted that the optimization could not transform 1T into the 2H phase but induce some distortions, indicating the activation barrier for the phase transformation is higher than the relaxation of the boundary. In addition, the atomic network can be subjected to strain as a result of defects in the phase boundary. Fig. S3 shows the strain map, which is specified as the total displacements in all three axes as compared to the perfect interface. It can be seen that the largest change in the atomic positions occurs in the case of V_{Mo+3S} at the interfaces while the sulfur vacancies induce the smallest displacements into the phase boundary.

3.1 Sulfur vacancies

In this section, we present the electronic and transport properties of T-H heterophase junction containing interfacial sulfur vacancies; V_S , V_{2S-top} , and V_{2S-par} . In Fig. 2, local density of states (LDOS) on the atoms at the left interface of such devices are plotted at Bias = 0.00 V and Bias = 1.40 V. In the following, the term "interface" is used for a part of the device, which consists of atoms from one layer of 1T-MoS₂ and one layer of 2H-MoS₂. Due to the electronic states from T phase, the band gap in LDOS is narrower than that for pristine 2H phase of MoS₂. Comparing the two figures, there is a shift in the energy, corresponding

to half of the applied voltage.

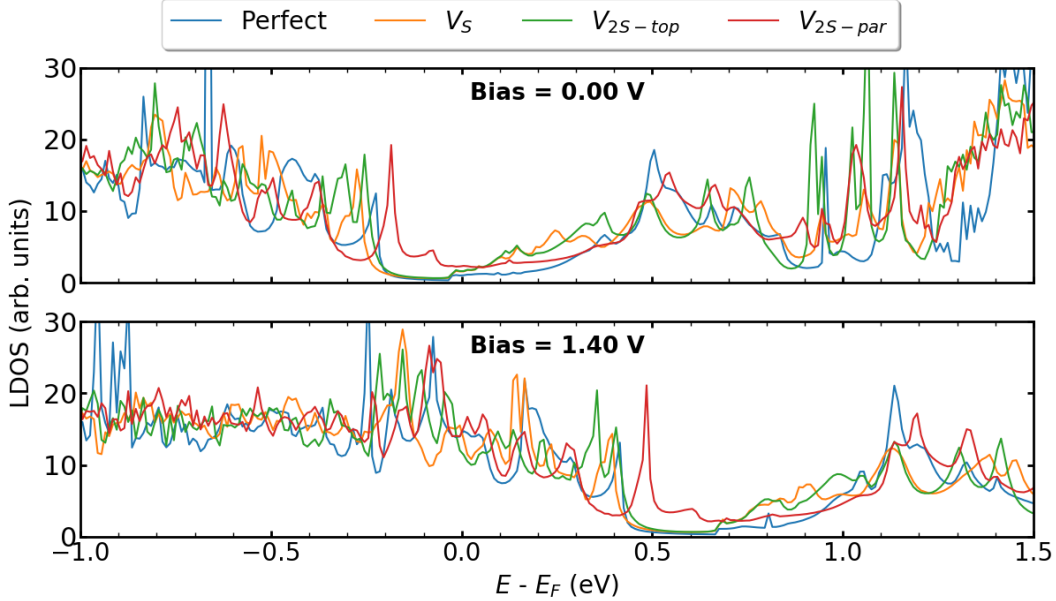


Figure 2: (Color online) LDOS at the left interface of T-H heterophase junction containing various sulfur vacancies; V_S , V_{2S-top} , and V_{2S-par} . Energies are shifted with respect to their corresponding Fermi energy.

The presence of defects introduces new states close to the Fermi level and increases electron density at the interface, which is mainly contributed by metal d orbitals. It is evident that defect-associated states are more pronounced in the case of V_{2s-par} where the electron density is enhanced in the vicinity of the Fermi level, including a peak at -0.2 eV. The results showed that other types of sulfur vacancies have a negligible impact on the electronic structure around the Fermi energy. It should be noted that the sulfur vacancies in 2H-MoS₂ monolayers act as scattering centers and consequently diminish the transport properties [25–28].

In order to elaborate the electron conduction dependency on the geometry of contact between the T and the H phases, transmission spectra for the junction without and with interfacial defects at two Bias, 0.00 and 1.40 V, are shown in Fig. 3a and 3b, respectively. Corresponding to the band gap of 2H-MoS₂, there is no transmission at zero bias within an energy range of 1.7 eV around the Fermi level. A comparison between perfect interface and those containing sulfur vacancies shows a growth in transmission probability, suggesting the

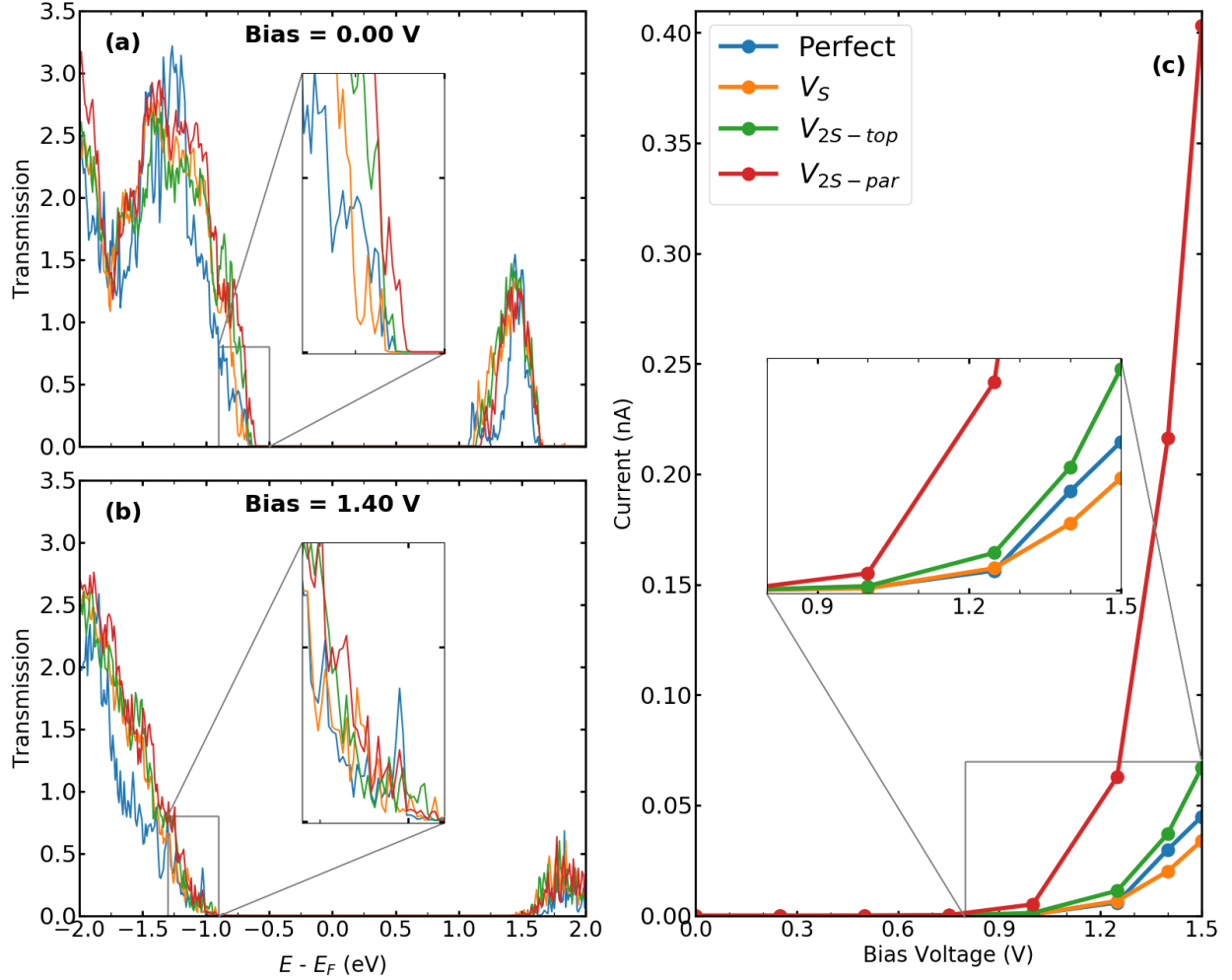


Figure 3: (Color online) Transmission spectra for T-H heterophase junction of MoS₂ monolayer containing various sulfur vacancies at both interfaces at a) Bias = 0.00 V and b) Bias = 1.40 V. Energies are shifted with respect to their corresponding Fermi energy. The insets show the change in the electronic transmission channels at the top of the valance band. c) I-V characteristics for the same devices. The inset shows the current around the threshold voltage.

contribution of defect states in electrical transport. Specifically, the transmission coefficients close to the valance band edge can be increased to almost two times for the case of V_{2S-par} vacancy. The IV characteristics of the studied T-H heterophase junction are shown in Fig. 3c. The junction displays a non-linear current-voltage similar to the characteristics of a resonant tunneling diode. The energy mismatch between the Fermi energy of the metallic

1T electrodes and the lowest unoccupied levels of the 2H phase causes the presence of zero current and the need for threshold voltage to produce finite current flow through the junction. The value of threshold voltage was reduced from 1.0 V for the perfect interface to 0.75V for the interface with divacancy. The appearance of defect-associated resonant states in the transmission spectra within the voltage window changes the current through the system, leading to an increase by an order of magnitude, when V_{2S-par} vacancy is present at the interfaces, as shown in Fig. 3c.

3.2 Molybdenum vacancies and vacancy complexes

We calculate the electronic and transport properties of the T-H heterophase junction when molybdenum vacancy, V_{Mo} , and vacancy complexes V_{Mo+3S} and V_{Mo+6S} are present at the interface. The LDOS of the interface is shown in Fig. 4 at Bias = 0.00 V and Bias = 1.40 V. Here, the applied bias has shifted the energies. The electronic structure of the interfaces with a single Mo vacancy varies more than that of a single sulfur vacancy. In the case of larger point defects, i.e. V_{Mo+6S} , the electronic structure shows several resonant states around the Fermi level which are mainly formed by Mo 4d states. The defect-induced changes in the electronic structure affect the carrier injection through the junction. The transmission function (Fig. 5b&c) at the top of the valance band shows a significant enhancement when vacancies are introduced into the interfaces. Accordingly, the current is increased by up to three orders of magnitude in comparison to the perfect interface. This is due to an enhancement of carrier occupations near the Fermi level, which leads to an increase in the transmission spectrum. As a result, the interfaces with V_{Mo+6S} vacancy demonstrate a threshold voltage of 0.5 V, half of that for a perfect interface.

To further investigate the transport behaviour at the interface, we also plot the vector current for perfect systems and devices with V_{Mo} at both interfaces (Fig. S4). Vector current displays the direction and the amount of current, coming from the left or right electrode, projected on each atom and at a specific energy channel. While the perfect interface shows dominant current scattering at the T-H boundary for low bias voltages, e.g. V=-0.5 V, the currents are delocalized in the channel region with V_{Mo} at the interface, suggesting that electrons have been well transmitted from electrodes to the channel region.

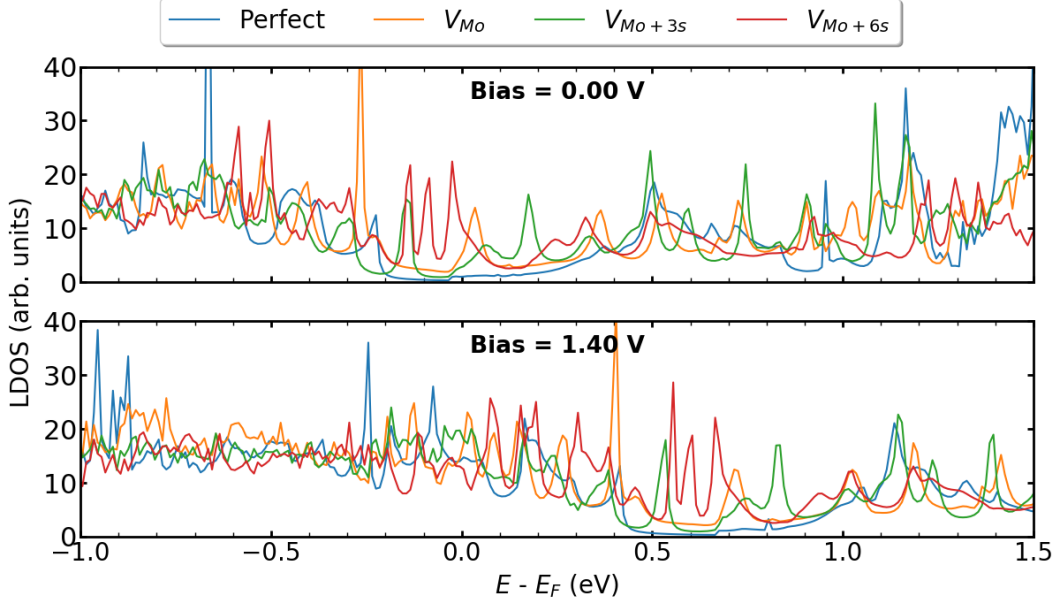


Figure 4: (Color online) LDOS at the left interface of T-H heterophase junction containing molybdenum vacancy, V_{Mo} , and vacancy complexes as V_{Mo+3s} and V_{Mo+6s} . Energies are shifted with respect to their corresponding Fermi energy.

We have also studied the influence of defect concentrations on the transport properties through the interfaces. Here, we fixed the length of the channel but varied its width, including the interfaces with a single V_{Mo} . Fig. ?? shows the difference in the conductance through devices ($\Delta G = G_{defect} - G_{perfect}$) as a function of the devices' areas. It is evident that the conductance reduces with decreasing the defect concentration approaching the value of the perfect interface for zero-defect density. Variation of channel widths has two different effects on the transport properties: On one hand, the number of transport channels increases with the width of the channel. On the other hand, for a constant number of defect sites, increasing the channel width leads to a decrease in the carrier densities around the Fermi Level. The former effect is canceled out by subtracting the conductivity of the system from the corresponding one with the pristine interface. As a result, for wider channels (lower concentrations), the increase in electrical conductivity is linearly reduced.

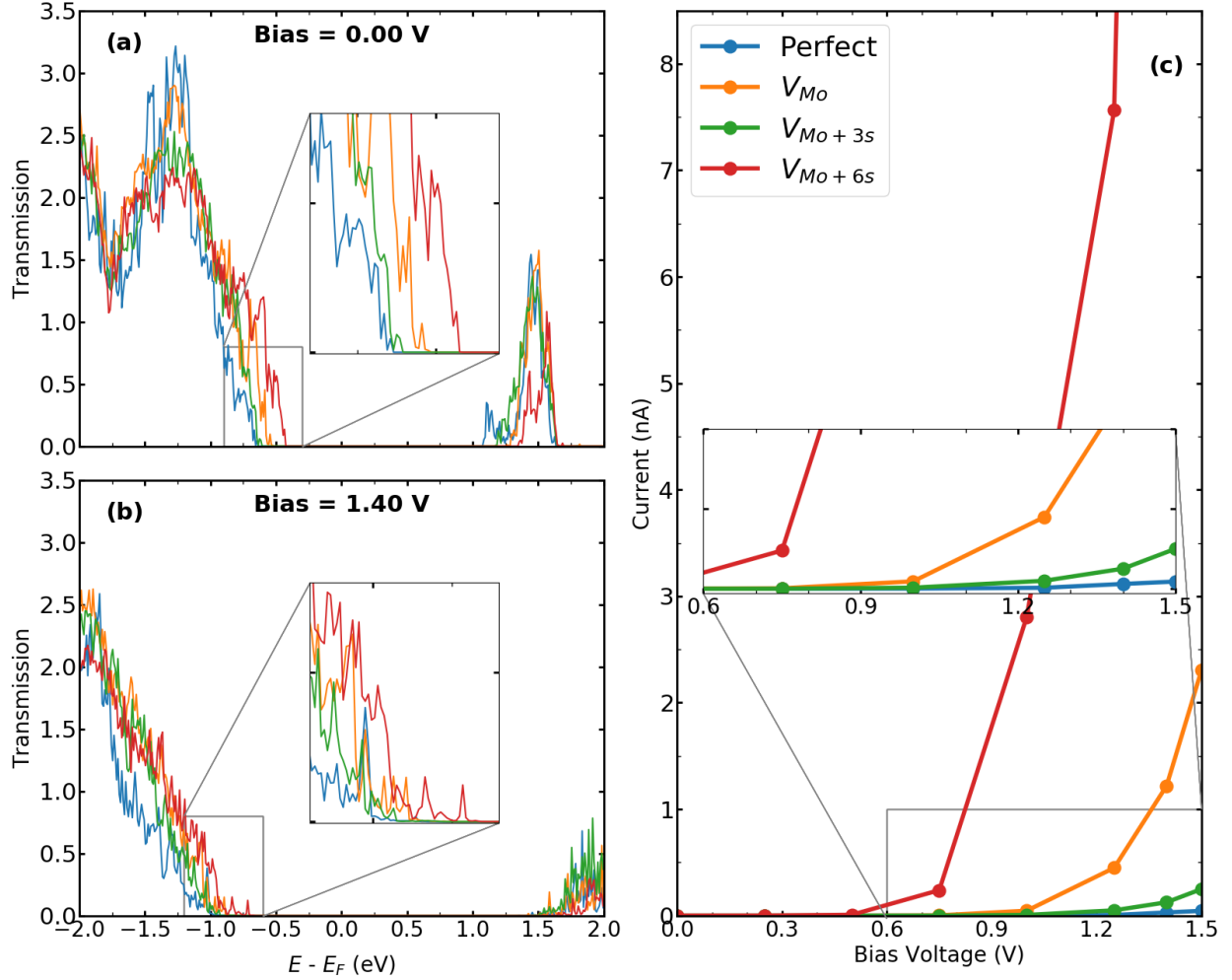


Figure 5: (Color online) Transmission spectra for T-H heterophase junction of MoS₂ monolayer containing molybdenum vacancy, V_{Mo} , and vacancy complexes as V_{Mo+3S} and V_{Mo+6S} at both interfaces at a) Bias = 0.00 V and b) Bias = 1.40 V. Energies are shifted with respect to their corresponding Fermi energy. The insets show the change in the electronic transmission channels at the top of the valance band. c) I-V characteristics for the same devices. The inset shows the current around the threshold voltage.

3.3 Antisites

Because vacancy and antisite are both high electron-scattering centers, their presence in TMDs can impair sample mobility [52]. We further investigate the influence of antisites defects, such as MoS , Mo_{2S-top} , S_{Mo} , and $2S-top_{Mo}$, at the interfaces of T-H heterophase

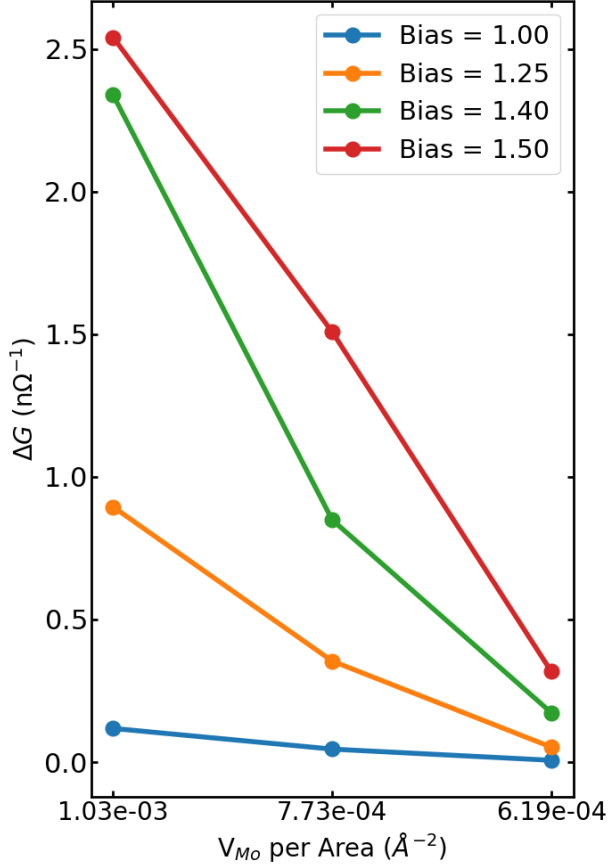


Figure 6: (Color online) Difference in the conductance through perfect systems and device with V_{Mo} ($\Delta G = G_{defect} - G_{perfect}$) as function of the device's area at different bias voltages. Since number of vacancies is the same for all cases, it is also a function of the defect density. It is true that more transport channels are added to wider devices, however, at the same time defect density is reduced, hence, decreasing the current through defective devices. Thus, conductance difference is approaching to zero, as the system gets wider.

junctions. Among all the considered antisites, the situation where molybdenum vacancy is substituted with two sulfurs ($2S - top_{Mo}$) provides the most pronounced defect associated states at the valence band edge (Fig. 7). When compared with the Mo vacancy, the defect states are more localized and originated mainly from hybridization between the Mo_d-S_p orbitals. The contributing orbitals to the LDOS at the left interface are shown in Fig. S5 in the supplementary information.

In Fig. 8a,b, transmission spectra for phase-engineered devices based on MLs MoS_2 , containing various substitutions, are displayed at Bias = 0.00 & 1.40 V. Fig. 8c shows the corresponding IV characteristics as a function of bias voltages up to 1.50V. When vacancies are substituted with sulfur or molybdenum atoms, the current stays in the same order as for the device with perfect interfaces. Only for the case of $2S - top_{Mo}$, current has been

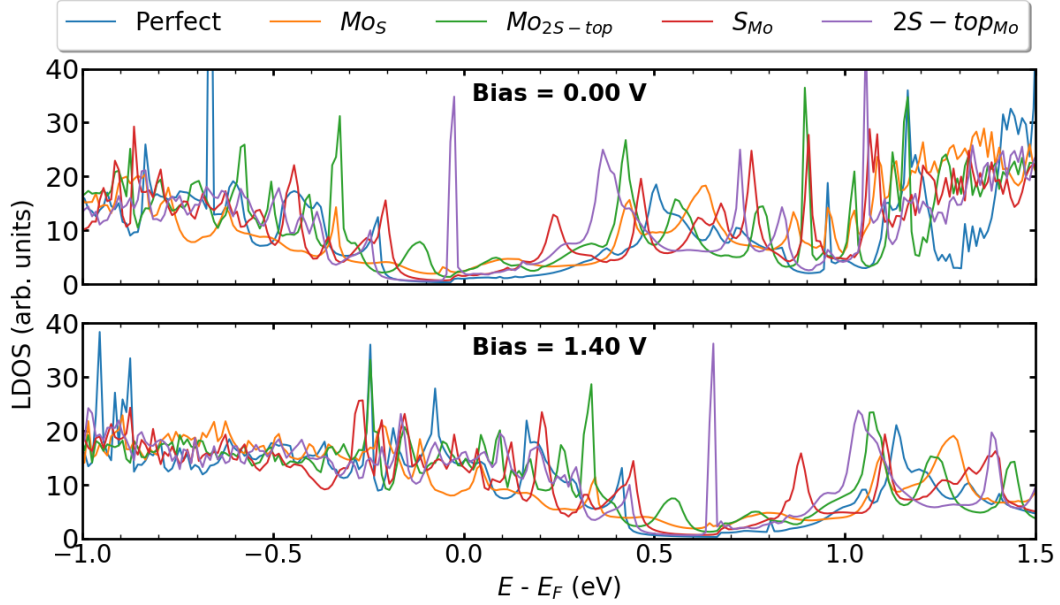


Figure 7: (Color online) LDOS at the left interface of T-H heterophase junction containing various substitutions; MoS , Mo_{2S-top} , S_{Mo} , $2S-top_{Mo}$. Energies are shifted with respect to their corresponding Fermi energy.

slightly increased due to the presence of midgap defect states observed in LDOS and the enhancement in the transmission probabilities. It's also worth noting that, in contrast to the case of perfect interfaces, the presence of antisite defects inevitably results in more phonon scattering channels, which may be beneficial in lowering lattice thermal conductivity.

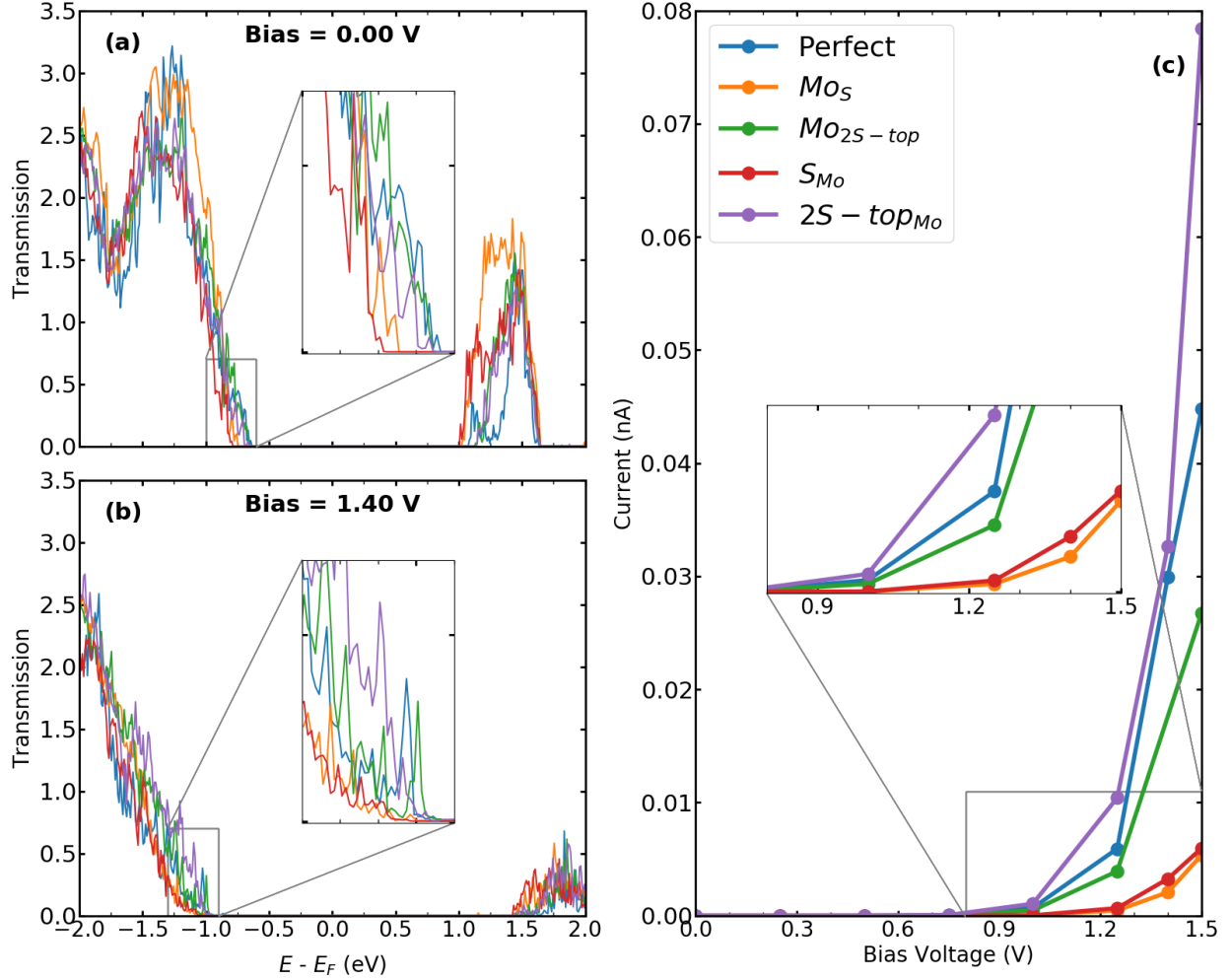


Figure 8: (Color online) Transmission spectra for T-H heterophase junction of MoS₂ monolayer containing various substitutions; MoS , Mo_{2S-top} , S_{Mo} , $2S-top_{Mo}$, at both interfaces at a) Bias = 0.00 V and b) Bias = 1.40 V. Energies are shifted with respect to their corresponding Fermi energy. The insets show the change in the electronic transmission channels at the top of the valance band. c) I-V characteristics for the same devices. The inset shows the current around the threshold voltage.

4 Conclusion

In the present paper, transport properties of charge carriers through devices based on metallic (1T) and Semiconductor (2H) phases of MoS₂ monolayers are investigated. Various point defects are present at both interfaces: V_S , V_{2S-top} , V_{2S-par} , V_{Mo} , V_{Mo+3S} , V_{Mo+6S} , MoS ,

Mo_{2S-top} , S_{Mo} , and $2S-top_{Mo}$. The first-principles simulations and NEGF technique are used to compute the LDOS, transmission curves, and IV characteristics of perfect and defective devices under bias in the range of 0.00 V till 1.50 V. Our systematic study shows that defects at the interfaces provide the opportunity for further improvement of the transport properties of such devices. More notably, we found that transport properties are enhanced in the presence of energetically favorable intrinsic point defects. In contrast to the scattering character of defects in 2H-phase MoS₂, at the interface, they lead to emergence of resonant states close to the Fermi level, thereby giving rise to the enhancement of the current flow. In particular, creating a molybdenum vacancy induces defect midgap states in the LDOS and improves the transport characteristics, which, in turn, leads to an increase in the current up to two orders of magnitude. The knowledge developed in this study could pave the way for the promising applications of lateral heterojunctions of 1T/2H MoS₂ monolayers in field effect devices.

Author Contributions

Conceptualization, M.B. and M.G.-A; investigation, M.B.; methodology, M. B., and M.G.-A.; writing, M.B., M.G.-A., T. F.; supervision, M. G.-A, T. F. All authors have read and agreed to the published version of the manuscript.

Conflicts of interest

There are no conflicts to declare.

Acknowledgements

We thank the DFG funded research training group "GRK 2247".M.B. acknowledges the support provided by DAAD and the PIP program at Bremen university. M.B. also thanks Dr. Nick Papior for his support during the transport calculations and Dr. Miguel Pruneda for his help to produce well-performed basis-sets and pseudopotentials.

References

- [1] O Ávalos-Ovando, D Mastrogiuseppe, and S E Ulloa. Lateral heterostructures and one-dimensional interfaces in 2D transition metal dichalcogenides. *Journal of Physics: Condensed Matter*, 31(21):213001, may 2019. ISSN 0953-8984. doi: 10.1088/1361-648X/ab0970. URL <http://stacks.iop.org/0953-8984/31/i=21/a=213001?key=crossref.5a9885b95b345c29fe4a591bcf8af511>. 2
- [2] Jianwei Wang, Zhiqiang Li, Haiyuan Chen, Guangwei Deng, and Xiaobin Niu. Recent Advances in 2D Lateral Heterostructures, dec 2019. ISSN 21505551. URL <https://doi.org/10.1007/s40820-019-0276-y>.
- [3] Michel Houssa, Ruishen Meng, Valery Afanas'ev, and André Stesmans. First-principles study of the contact resistance at 2D metal/2D semiconductor heterojunctions, apr 2020. ISSN 20763417. URL www.mdpi.com/journal/applsci. 2
- [4] Manish Chhowalla, Hyeon Suk Shin, Goki Eda, Lain Jong Li, Kian Ping Loh, and Hua Zhang. The chemistry of two-dimensional layered transition metal dichalcogenide nanosheets, apr 2013. ISSN 17554330. 2
- [5] Amirhasan Nourbakhsh, Ahmad Zubair, Redwan N. Sajjad, Tavakkoli K.G. Amir, Wei Chen, Shiang Fang, Xi Ling, Jing Kong, Mildred S. Dresselhaus, Efthimios Kaxiras, Karl K. Berggren, Dimitri Antoniadis, and Tomás Palacios. MoS₂ Field-Effect Transistor with Sub-10 nm Channel Length. *Nano Letters*, 16(12):7798–7806, dec 2016. ISSN 15306992. doi: 10.1021/acs.nanolett.6b03999. 2
- [6] D. Marian, E. Dib, T. Cusati, A. Fortunelli, G. Iannaccone, and G. Fiori. Two-dimensional transistors based on MoS₂ lateral heterostructures. In *Technical Digest - International Electron Devices Meeting, IEDM*, pages 14.1.1–14.1.4. IEEE, dec 2017. ISBN 9781509039012. doi: 10.1109/IEDM.2016.7838413. URL <http://ieeexplore.ieee.org/document/7838413/>. 2, 6
- [7] Yung Chang Lin, Dumitru O. Dumcenco, Ying Sheng Huang, and Kazu Suenaga. Atomic mechanism of the semiconducting-to-metallic phase transition in single-layered

- MoS₂. *Nature Nanotechnology*, 9(5):391–396, apr 2014. ISSN 17483395. doi: 10.1038/nnano.2014.64. URL www.nature.com/naturenanotechnology. 2
- [8] Rajesh Kappera, Damien Voiry, Sibel Ebru Yalcin, Brittany Branch, Gautam Gupta, Aditya D. Mohite, and Manish Chhowalla. Phase-engineered low-resistance contacts for ultrathin MoS₂ transistors. *Nature Materials*, 13(12):1128–1134, dec 2014. ISSN 1476-1122. doi: 10.1038/nmat4080. URL <http://www.nature.com/articles/nmat4080>. 2
- [9] Suyeon Cho, Sera Kim, Jung Ho Kim, Jiong Zhao, Jinbong Seok, Dong Hoon Keum, Jaeyoon Baik, Duk Hyun Choe, K. J. Chang, Kazu Suenaga, Sung Wng Kim, Young Hee Lee, and Heejun Yang. Phase patterning for ohmic homojunction contact in MoTe₂. *Science*, 349(6248):625–628, aug 2015. ISSN 10959203. doi: 10.1126/science.aab3175. 2
- [10] Jiahao Kang, Wei Liu, Deblina Sarkar, Debdeep Jena, and Kaustav Banerjee. Computational study of metal contacts to monolayer transition-metal dichalcogenide semiconductors, jul 2014. ISSN 21603308. URL <https://link.aps.org/doi/10.1103/PhysRevX.4.031005>. 2
- [11] Yierpan Aierken, Cem Sevik, Ouz Gülseren, François M. Peeters, and Deniz Çakir. In pursuit of barrierless transition metal dichalcogenides lateral heterojunctions. *Nanotechnology*, 29(29), may 2018. ISSN 13616528. doi: 10.1088/1361-6528/aac17d. 3, 4
- [12] Zhi Qiang Fan, Xiang Wei Jiang, Jiezhi Chen, and Jun Wei Luo. Improving Performances of In-Plane Transition-Metal Dichalcogenide Schottky Barrier Field-Effect Transistors. *ACS Applied Materials and Interfaces*, 10(22):19271–19277, jun 2018. ISSN 19448252. doi: 10.1021/acsami.8b04860. URL <http://pubs.acs.org/doi/10.1021/acsami.8b04860>. 2, 3
- [13] Xiang Zhang, Zehua Jin, Luqing Wang, Jordan A. Hachtel, Eduardo Villarreal, Zixing Wang, Teresa Ha, Yusuke Nakanishi, Chandra Sekhar Tiwary, Jiawei Lai, Liangliang

- Dong, Jihui Yang, Robert Vajtai, Emilie Ringe, Juan Carlos Idrobo, Boris I. Yakobson, Jun Lou, Vincent Gambin, Rachel Koltun, and Pulickel M. Ajayan. Low Contact Barrier in 2H/1T MoTe₂ In-Plane Heterostructure Synthesized by Chemical Vapor Deposition. *ACS Applied Materials and Interfaces*, 11(13):12777–12785, apr 2019. ISSN 19448252. doi: 10.1021/acsami.9b00306. [2](#)
- [14] Adam L. Friedman, F. Keith Perkins, Aubrey T. Hanbicki, James C. Culbertson, and Paul M. Campbell. Dynamics of chemical vapor sensing with MoS₂ using 1T/2H phase contacts/channel. *Nanoscale*, 8(22):11445–11453, jun 2016. ISSN 2040-3364. doi: 10.1039/C6NR01979J. URL <http://xlink.rsc.org/?DOI=C6NR01979J>. [2](#)
- [15] Hannu-Pekka Komsa, Simon Kurasch, Ossi Lehtinen, Ute Kaiser, and Arkady V Krasheninnikov. From point to extended defects in two-dimensional MoS₂: Evolution of atomic structure under electron irradiation. *Physical Review B*, 88(035301), 2013. doi: 10.1103/PhysRevB.88.035301. URL <https://journals.aps.org/prb/pdf/10.1103/PhysRevB.88.035301>. [2](#), [6](#)
- [16] Xiaonian Yang, Qiang Li, Guofeng Hu, Zegao Wang, Zhenyu Yang, Xingqiang Liu, Mingdong Dong, and Caofeng Pan. Controlled synthesis of high-quality crystals of monolayer MoS₂ for nanoelectronic device application. *Science China Materials*, 59(3): 182–190, mar 2016. ISSN 2199-4501. doi: 10.1007/s40843-016-0130-1. URL <https://doi.org/10.1007/s40843-016-0130-1>. [5](#)
- [17] Sang Wook Han, Youngsin Park, Young Hun Hwang, Soyoung Jekal, Manil Kang, Wang G. Lee, Woochul Yang, Gun Do Lee, and Soon Cheol Hong. Electron beam-formed ferromagnetic defects on MoS₂ surface along 1 T phase transition. *Scientific Reports*, 6(1):1–8, dec 2016. ISSN 20452322. doi: 10.1038/srep38730. URL www.nature.com/scientificreports/. [6](#)
- [18] Mahdi Ghorbani-Asl, Silvan Kretschmer, Douglas E Spearot, and Arkady V Krasheninnikov. Two-dimensional MoS₂ under ion irradiation: from controlled defect production to electronic structure engineering. *2D Materials*, 4(2):025078, apr 2017.

- doi: 10.1088/2053-1583/aa6b17. URL <http://stacks.iop.org/2053-1583/4/i=2/a=025078?key=crossref.2fecafdf5741bc0339eabdee76e4b01e>.
- [19] L. Ma, Y. Tan, M. Ghorbani-Asl, R. Boettger, S. Kretschmer, S. Zhou, Z. Huang, A. V. Krasheninnikov, and F. Chen. Tailoring the optical properties of atomically-thin WS₂: Via ion irradiation. *Nanoscale*, 9(31):11027–11034, aug 2017. ISSN 20403372. doi: 10.1039/c7nr02025b. URL <http://xlink.rsc.org/?DOI=C7NR02025B>. 6
- [20] J. Klein, M. Lorke, M. Florian, F. Sigger, L. Sigl, S. Rey, J. Wierzbowski, J. Cerne, K. Müller, E. Mitterreiter, P. Zimmermann, T. Taniguchi, K. Watanabe, U. Wurstbauer, M. Kaniber, M. Knap, R. Schmidt, J. J. Finley, and A. W. Holleitner. Site-selectively generated photon emitters in monolayer MoS₂ via local helium ion irradiation. *Nature Communications*, 10(1):2755, dec 2019. ISSN 2041-1723. doi: 10.1038/s41467-019-10632-z. URL <http://www.nature.com/articles/s41467-019-10632-z>. 6
- [21] K. Barthelmi, J. Klein, A. Hötger, L. Sigl, F. Sigger, E. Mitterreiter, S. Rey, S. Gyger, M. Lorke, M. Florian, F. Jahnke, T. Taniguchi, K. Watanabe, V. Zwiller, K. D. Jöns, U. Wurstbauer, C. Kastl, A. Weber-Bargioni, J. J. Finley, K. Müller, and A. W. Holleitner. Atomistic defects as single-photon emitters in atomically thin MoS₂, aug 2020. ISSN 00036951. URL <http://aip.scitation.org/doi/10.1063/5.0018557>.
- [22] Elmar Mitterreiter, Bruno Schuler, Katja Barthelmi, Katherine Cochrane, Jonas Kiemle, Florian Sigger, Julian Klein, Ed Wong, Edward Barnard, Sivan Refaely-Abramson, Diana Qiu, Michael Lorke, Frank Jahnke, Jonathan Finley, T U Muenchen, and Adam Schwartzberg. The role of chalcogen vacancies for atomic defect emission in MoS₂. nov 2020. doi: 10.21203/rs.3.rs-105682/v1. URL <https://www.researchsquare.com/article/rs-105682/v1>. 2
- [23] Silvan Kretschmer, Hannu Pekka Komsa, Peter Bøggild, and Arkady V Krasheninnikov. Structural Transformations in Two-Dimensional Transition-Metal Dichalcogenide MoS₂ under an Electron Beam: Insights from First-Principles Calculations. *Journal of Physical Chemistry Letters*, 8(13):3061–3067, 2017. ISSN 19487185. doi:

- 10.1021/acs.jpcllett.7b01177. URL <https://pubs.acs.org/doi/pdf/10.1021/acs.jpcllett.7b01177>. 2
- [24] Jianqi Zhu, Zhichang Wang, Hua Yu, Na Li, Jing Zhang, JianLing Meng, Mengzhou Liao, Jing Zhao, Xiaobo Lu, LuoJun Du, Rong Yang, Dongxia Shi, Ying Jiang, and Guangyu Zhang. Argon Plasma Induced Phase Transition in Monolayer MoS₂. *Journal of the American Chemical Society*, 139(30):10216–10219, aug 2017. ISSN 15205126. doi: 10.1021/jacs.7b05765. URL <http://pubs.acs.org/doi/10.1021/jacs.7b05765>. 2
- [25] Mahdi Ghorbani-Asl, Andrey N Enyashin, Agnieszka Kuc, Gotthard Seifert, and Thomas Heine. Defect-induced conductivity anisotropy in MoS₂ monolayers. *Physical Review B*, 8820, 2013. doi: 10.1103/PhysRevB.88.245440. URL <https://journals.aps.org/prb/pdf/10.1103/PhysRevB.88.245440>. 2, 7
- [26] Mohnish Pandey, Filip A. Rasmussen, Korina Kuhar, Thomas Olsen, Karsten W. Jacobsen, and Kristian S. Thygesen. Defect-Tolerant Monolayer Transition Metal Dichalcogenides. *Nano Letters*, 16(4):2234–2239, apr 2016. ISSN 1530-6984. doi: 10.1021/acs.nanolett.5b04513. URL <http://pubs.acs.org/doi/pdf/10.1021/acs.nanolett.5b04513><http://pubs.acs.org/doi/10.1021/acs.nanolett.5b04513>.
- [27] Zhong Lin, Bruno R Carvalho, Ethan Kahn, Ruitao Lv, Rahul Rao, Humberto Terrones, Marcos A Pimenta, and Mauricio Terrones. Defect engineering of two-dimensional transition metal dichalcogenides, apr 2016. ISSN 20531583. URL <http://stacks.iop.org/2053-1583/3/i=2/a=022002?key=crossref.80d7e4936acbe766cd2f8cae3076a74e>. 6
- [28] Mohammad Bahmani, Mahdi Faghinasiri, Michael Lorke, Agnieszka Beata Kuc, and Thomas Frauenheim. Electronic Properties of Defective MoS₂ Monolayers Subject to Mechanical Deformations: A First-Principles Approach. *Physica Status Solidi (B) Basic Research*, page 1900541, mar 2020. ISSN 15213951. doi: 10.1002/pssb.201900541. URL <https://onlinelibrary.wiley.com/doi/abs/10.1002/pssb.201900541>. 2, 6, 7
- [29] K S Novoselov, D Jiang, F Schedin, T J Booth, V V Khotkevich, S V Morozov, and A K Geim. Two-dimensional atomic crystals. *Proceedings of the National*

- Academy of Sciences*, 102(30):10451–10453, jul 2005. ISSN 0027-8424. doi: 10.1073/pnas.0502848102. URL <http://www.ncbi.nlm.nih.gov/pubmed/16027370><http://www.pubmedcentral.nih.gov/articlerender.fcgi?artid=PMC1180777>. 3
- [30] B. Radisavljevic, A. Radenovic, J. Brivio, V. Giacometti, and A. Kis. Single-layer MoS₂ transistors. *Nature Nanotechnology*, 6(3):147–150, mar 2011. ISSN 1748-3387. doi: 10.1038/nnano.2010.279. URL <http://www.nature.com/doifinder/10.1038/nnano.2010.279>.
- [31] Yi Hsien Lee, Xin Quan Zhang, Wenjing Zhang, Mu Tung Chang, Cheng Te Lin, Kai Di Chang, Ya Chu Yu, Jacob Tse Wei Wang, Chia Seng Chang, Lain Jong Li, and Tsung Wu Lin. Synthesis of large-area MoS₂ atomic layers with chemical vapor deposition. *Advanced Materials*, 24(17):2320–2325, may 2012. ISSN 09359648. doi: 10.1002/adma.201104798. URL <http://doi.wiley.com/10.1002/adma.201104798>. 3
- [32] Kian Soon Yong, Diana M. Otalvaro, Ivan Duchemin, Mark Saeys, and Christian Joachim. Calculation of the conductance of a finite atomic line of sulfur vacancies created on a molybdenum disulfide surface. *Physical Review B - Condensed Matter and Materials Physics*, 77(20):205429, may 2008. ISSN 10980121. doi: 10.1103/PhysRevB.77.205429. URL <https://journals.aps.org/prb/abstract/10.1103/PhysRevB.77.205429>. 3
- [33] Ziyu Hu, Shengli Zhang, Yan Ning Zhang, Da Wang, Haibo Zeng, and Li Min Liu. Modulating the phase transition between metallic and semiconducting single-layer MoS₂ and WS₂ through size effects. *Physical Chemistry Chemical Physics*, 17(2):1099–1105, jan 2015. ISSN 14639076. doi: 10.1039/c4cp04775c. 3, 4
- [34] Ganesh Sivaraman, Fábio A.L. De Souza, Rodrigo G. Amorim, Wanderlã L. Scopel, Maria Fyta, and Ralph H. Scheicher. Electronic Transport along Hybrid MoS₂ Monolayers. *Journal of Physical Chemistry C*, 120(41):23389–23396, oct 2016. ISSN 19327455. doi: 10.1021/acs.jpcc.6b07917. URL <https://pubs.acs.org/doi/10.1021/acs.jpcc.6b07917>. 4

- [35] Zhi Qiang Fan, Xiang Wei Jiang, Jun Wei Luo, Li Ying Jiao, Ru Huang, Shu Shen Li, and Lin Wang Wang. In-plane Schottky-barrier field-effect transistors based on 1 T /2 H heterojunctions of transition-metal dichalcogenides. *Physical Review B*, 96(16):165402, oct 2017. ISSN 24699969. doi: 10.1103/PhysRevB.96.165402. URL <https://link.aps.org/doi/10.1103/PhysRevB.96.165402>.
- [36] Damiano Marian, Elias Dib, Teresa Cusati, Enrique G. Marin, Alessandro Fortunelli, Giuseppe Iannaccone, and Gianluca Fiori. Transistor Concepts Based on Lateral Heterostructures of Metallic and Semiconducting Phases of MoS₂. *Physical Review Applied*, 8(5):054047, nov 2017. ISSN 2331-7019. doi: 10.1103/PhysRevApplied.8.054047. URL <https://link.aps.org/doi/10.1103/PhysRevApplied.8.054047>. 3
- [37] Pablo Ordejon, Emilio Artacho, and Jose M. Soler. Selfconsistent order-N density-functional calculations for very large systems. *Physical Review B*, 53(16):R10441–R10444, apr 1996. ISSN 0163-1829. doi: 10.1103/PhysRevB.53.R10441. URL <https://link.aps.org/doi/10.1103/PhysRevB.53.R10441><http://arxiv.org/abs/cond-mat/9601002><http://dx.doi.org/10.1103/PhysRevB.53.R10441>. 3
- [38] José M Soler, Emilio Artacho, Julian D Gale, Alberto García, Javier Junquera, Pablo Ordejón, and Daniel Sánchez-Portal. The SIESTA method for ab initio order-N materials simulation. *Journal of Physics Condensed Matter*, 14(11):2745–2779, mar 2002. ISSN 09538984. doi: 10.1088/0953-8984/14/11/302. URL <http://stacks.iop.org/0953-8984/14/i=11/a=302?key=crossref.8ed2406c09184bcd143191af26e9f492>. 3
- [39] N. Troullier and José Luriaas Martins. Efficient pseudopotentials for plane-wave calculations. *Physical Review B*, 43(3):1993–2006, jan 1991. doi: 10.1103/PhysRevB.43.1993. URL <https://link.aps.org/doi/10.1103/PhysRevB.43.1993>. 3
- [40] N. Troullier and José Luriaas Martins. Efficient pseudopotentials for plane-wave calculations. II. Operators for fast iterative diagonalization. *Physical Review B*, 43(11):8861–8869, apr 1991. ISSN 01631829. doi: 10.1103/PhysRevB.43.8861. URL <https://link.aps.org/doi/10.1103/PhysRevB.43.8861>. 3

- [41] John P. Perdew, Kieron Burke, and Matthias Ernzerhof. Generalized gradient approximation made simple. *Physical Review Letters*, 77(18):3865–3868, oct 1996. ISSN 00319007. doi: 10.1103/PhysRevLett.77.3865. URL <https://link.aps.org/doi/10.1103/PhysRevLett.77.3865>. 3
- [42] Mads Brandbyge, José Luis Mozos, Pablo Ordejón, Jeremy Taylor, and Kurt Stokbro. Density-functional method for nonequilibrium electron transport. *Physical Review B - Condensed Matter and Materials Physics*, 65(16):1654011–16540117, apr 2002. ISSN 01631829. doi: 10.1103/PhysRevB.65.165401. 4
- [43] Nick Papior, Nicolás Lorente, Thomas Frederiksen, Alberto García, and Mads Brandbyge. Improvements on non-equilibrium and transport Green function techniques: The next-generation TRANSIESTA. *Computer Physics Communications*, 212:8–24, mar 2017. ISSN 00104655. doi: 10.1016/j.cpc.2016.09.022. 4
- [44] Rolf Landauer. Electrical resistance of disordered one-dimensional lattices. *Philosophical Magazine*, 21(172):863–867, 1970. ISSN 00318086. doi: 10.1080/14786437008238472. 4
- [45] Mahdi Ghorbani-Asl, Paul D. Bristowe, and Krzysztof Koziol. A computational study of the quantum transport properties of a cucnt composite. *Phys. Chem. Chem. Phys.*, 17:18273–18277, 2015. doi: 10.1039/C5CP01470K. 5
- [46] Wu Zhou, Xiaolong Zou, Sina Najmaei, Zheng Liu, Yumeng Shi, Jing Kong, Jun Lou, Pulickel M Ajayan, Boris I Yakobson, and Juan Carlos Idrobo. Intrinsic structural defects in monolayer molybdenum disulfide. *Nano Letters*, 13(6):2615–2622, 2013. ISSN 15306984. doi: 10.1021/nl4007479. URL <https://pubs.acs.org/sharingguidelines>. 6
- [47] Michael G. Stanford, Yu-Chuan Lin, Maria Gabriela Sales, Anna N. Hoffman, Christopher T. Nelson, Kai Xiao, Stephen McDonnell, and Philip D. Rack. Lithographically patterned metallic conduction in single-layer MoS₂ via plasma processing. *npj 2D Materials and Applications*, 3(1):13, dec 2019. ISSN 2397-7132. doi: 10.1038/s41699-019-0095-5. URL <http://www.nature.com/articles/s41699-019-0095-5>. 6

- [48] Hannu-Pekka Komsa and Arkady V Krasheninnikov. Native defects in bulk and monolayer MoS₂ from first principles. *Physical Review B*, 91(125304), 2015. doi: 10.1103/PhysRevB.91.125304. URL <https://journals.aps.org/prb/pdf/10.1103/PhysRevB.91.125304>. 6
- [49] Rafael Roldán, Jose A. Silva-Guillén, M. Pilar López-Sancho, Francisco Guinea, Emanuele Cappelluti, and Pablo Ordejón. Electronic properties of single-layer and multilayer transition metal dichalcogenides MX₂ (M = Mo, W and X = S, Se), oct 2014. ISSN 15213889. URL <http://doi.wiley.com/10.1002/andp.201400128>.
- [50] Dipankar Saha and Santanu Mahapatra. Atomistic modeling of the metallic-to-semiconducting phase boundaries in monolayer MoS₂. *Applied Physics Letters*, 108(25), jun 2016. ISSN 00036951. doi: 10.1063/1.4954257.
- [51] Chithra H. Sharma, Ananthu P. Surendran, Abin Varghese, and Madhu Thalakulam. Stable and scalable 1T MoS₂ with low temperature-coefficient of resistance. *Scientific Reports*, 8(1):12463, dec 2018. ISSN 2045-2322. doi: 10.1038/s41598-018-30867-y. URL <http://www.nature.com/articles/s41598-018-30867-y>. 6
- [52] Jinhua Hong, Zhixin Hu, Matt Probert, Kun Li, Danhui Lv, Xinan Yang, Lin Gu, Nannan Mao, Qingliang Feng, Liming Xie, Jin Zhang, Dianzhong Wu, Zhiyong Zhang, Chuanhong Jin, Wei Ji, Xixiang Zhang, Jun Yuan, and Ze Zhang. Exploring atomic defects in molybdenum disulphide monolayers. *Nature Communications*, 6(1):6293, may 2015. ISSN 20411723. doi: 10.1038/ncomms7293. URL <http://www.nature.com/articles/ncomms7293>. 11